Smart Meter Pinging and Reading Through AMI Two-Way Communication Networks to Monitor Grid Edge Devices and DERs

Can Huang, *Senior Member, IEEE*, Chih-Che Sun, *Member, IEEE*, Nan Duan, *Senior Member, IEEE*, Yuming Jiang, *Senior Member, IEEE*, Chloe Applegate, Peter D. Barnes, Emma Stewart, *Senior Member, IEEE*

***Abstract*—Today's power distribution system is changing to a power-electronics-enabled distribution system, especially with the increasing penetration of distributed energy resources (DERs). To monitor and manage those electronic devices and DERs at the grid edge, the advanced metering infrastructure (AMI) with two-way communications presents great potentials. In the literature, extensive research explores the upstream communication from smart meters to electric utilities (e.g., meter reading) but few examine the downstream communication from the utilities to smart meters (e.g., meter pinging). This paper discussed the AMI two-way communication and its recent industrial practice in the U.S., especially the ones about applying the smart meter pinging functionality to monitor grid-edge devices and DERs. This paper then developed the two-way communication model and the network calculus method to quantify the impact of the two-way communication on the AMI network. In the end, the proposed method is validated with ns-3 simulation using the modified 13-node test feeder and real-world feeder systems.**

***Index Terms*—advanced metering infrastructure (AMI), distributed energy resources (DERs), network calculus, smart inverter, smart meter, time delay, two-way communications**

I. Introduction

TODAY'S electric power distribution system is developing from a passive network to an active network, especially with the increasing penetration of distributed energy resources (DERs). The active distribution system brings lots of benefits to electric utilities and end users, such as higher flexibility, resiliency, and sustainability [1], [2]. On the other hand, the distribution system is being involved with a large number of inverter- and converter-based devices and DERs, such as smart inverters and solar photovoltaic (PV), yielding a power-electronics-enabled distribution system [3]–[5]. It is thus critical to developing efficient resolutions to monitor and manage those devices and DERs at the grid edge [6].

Manuscript received November 5, 1999; revised February 3, 2000; accepted March 20, 2000. Date of publication March 25, 2000; date of current version August 19, 2000. Paper no. XXXX-01833-2020. (Corresponding author: Nan Duan.)

C. Huang, C. Sun, N. Duan, C. Applegate, and P. Barnes are with Lawrence Livermore National Laboratory, Livermore, 94550 CA, USA (e-mail: duan4@llnl.gov).

Y. Jiang is with the Department of Information Security and Communication Technology, Norwegian University of Science and Technology, 7491 Trondheim, Norway.

E. Stewart is with the National Rural Electric Cooperative Association, Arlington, VA 22203, USA.

Color versions of one or more figures in this article are available at https://doi.org/10.1109/XXXXX.2021.3069009.

Digital Object Identifier 10.1109/XXX.2021.3069009.

The mainstream measurement devices deployed at the distribution system are reviewed in the literature [7]–[9]. Among the various measurement devices, smart meters are the only measurement devices that are widely deployed between electric utilities and end users [10]–[12]. According to Energy Information Administration (EIA) report, the U.S. electric utilities had installed about 88 million smart meters at year-end 2018, covering nearly 70% of the U.S. households [13]. Smart meters along with their communications networks and meter data management systems (MDMS) constitute the advanced metering infrastructure (AMI), enabling automated, two-way communications between electric utilities and smart meters. Smart meters' wide deployment and two-way communication features present great potentials to address the monitoring and management issues of the grid edge devices and DERs. However, there are challenges ahead.

First, smart meters originally are designed for time-based rates, where many smart meters only record energy consumption data in kW or kW/h, without other readings (e.g., reactive power and voltage readings) [10]. The simple readings could not support advanced applications such as smart inverter and DER monitoring. Moreover, recently, several papers and reports summarized the functions, applications, and technology trends of smart meters [10]–[15]. They pointed out that it is advantageous to report energy consumption, together with real power, reactive power, and voltage measurements, such that smart meter data can be used for not only "load" billing and motioning, but also "grid edge" situational awareness; and it is also beneficial to explore new applications that extend the application scope from billing categories to monitoring and management categories, enabling smart meters' two-way communication feature to be fully utilized.

Second, since the historically passive nature of power distribution systems and the billing-based business model of AMI, most utilities invested in the AMI communication network with limited bandwidth and robustness. For example, in the U.S., 58% of residential smart meters, 28% commercial smart meters, and 10% of industrial smart meters reported meter reading in 30-minute or 1-hour time intervals, instead of 15-minute time intervals [10], [13]–[15], and many AMI systems still reply on 3G networks [13]–[15]. Therefore, smart meters' two-way communication feature has not been fully utilized. In the literature, extensive research explores the downstream from smart meters to electric utilities (e.g., smart meter reading), but few examine the upstream from electric utilities to end-

users (e.g., smart meter pinging) [10]–[15]. Moreover, there are few studies specifying the impact of adding additional data streams to smart meter datasets (e.g., voltage monitoring [15]) or applying advanced applications over the AMI network (e.g., DER and asset management [14]), especially in the communication perspective [14]–[20].

Currently, many AMI networks adopt wireless mesh networks (WMNs) to connect smart meters and cell relays [13]–[15]. In a WMN, some of smart meters need multiple hops to reach a cell relay, yielding a multi-hop wireless network. To study the quality of service (QoS), such as the end-to-end delay and package loss over a multi-hop wireless network, we need to consider many factors, including 1) the characteristics of the link, 2) how a link is shared and scheduled by users, 3) how a head-of-line (HoL) packet loss is handled at the medium access control (MAC) layer, and 4) the characteristics of the traffic. Generally, the first factor implies the data rate and loss rate on the link due to its characteristics. Depending on the used wireless communication technologies/standards, such as WiFi and WiMAX, the second factor can be highly different, which means different standards may deploy different approaches in a combination of the first factor. The third factor is determined by the standards. The fourth factor is mainly due to the applications. On the other hand, deterministic network calculus and stochastic network calculus are two major methods for network performance analysis [21]–[24]. The former is to compute and deduce a certain bound for service performance and provide a QoS guarantee, while the latter is based on the tail distribution of service capacity and provides a probabilistic QoS guarantee. Since most traditional smart meter applications are not time-critical, there is no research that applies deterministic or stochastic network calculus for AMI network performance analysis.

To this end, this work investigates the AMI network capability on monitoring and management of grid edge devices and DERs, and their potential impact on the AMI communication network. The major contributions are two-fold.

Theoretically, this work proposes the models of the AMI two-way communication network, including the downstream and the upstream. To identify the impact of adding smart inverter/DER data steams on the AMI network, this paper applies the network calculus method for the multi-hop mesh network. The network calculus results can help electric utilities quantify the impact of the new smart meter applications (e.g., smart inverter/DER monitoring) on the AMI network, with the metrics of the end-to-end delay, package loss, bandwidth usage, network congestion, etc.

Technically, this work is the first work that discusses smart meter pinging, which is a new smart meter function currently being deployed in engineering but seldom discussed in the literature. Smart meter pinging not only enables the AMI two-communication and closed-loop network to be fully utilized, but also enhances the monitoring and management of the power electronic devices and DERs at the grid edge. This study helps extend the smart meter application scope from "load" billing and motioning to "grid edge" situational awareness.

The remainder of this paper is organized as follows: Section II discusses the AMI two-way communication and its recent industrial practice; Section III provides the AMI two-way communication model; Section IV proposes the network calculus method; Section V validates the proposed model and method with case studies; Finally, a conclusion and future work are drawn in Section VI.

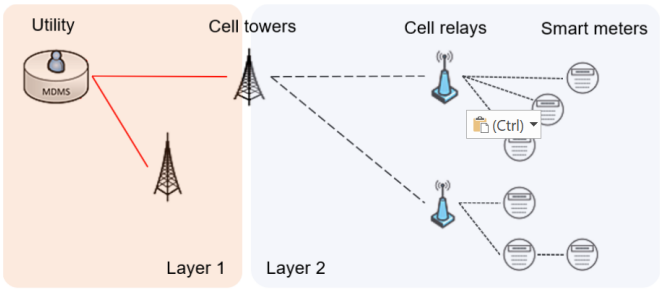

Fig. 1. A typical AMI.

II. AMI Two-Way Communication and Its Industry Applications

Since the first federal policy on advanced metering (i.e., EPAct 2005) was enacted in the U.S. in 2005, AMI has been rapidly developed and deployed throughout the country [13]. Compared with automatic meter reading (AMR), the breakthrough of AMI is the two-way communication [14]. In this section, the AMI two-way communication and its recent industrial practice are discussed, especially the ones about applying smart meter pinging and reading functionalities to monitor grid edge devices and DERs.

A. AMI Two-Way Communication

AMI is defined as an integrated system of smart meters, communications networks, and MDMSs with automated, two-way communications between utilities and customers [13]. A typical AMI communication network is depicted in Fig. 1, which consists of two layers. The first layer mainly connects intermediate data collection points (e.g., cell towers) with utilities, and the second layer connects the other intermediate collection points (e.g., cell relays) with smart meters. The communications between smart meters and utilities are bidirectional. On the upstream path, smart meter data are sent to utilities for billing and monitoring purposes, whereas on the downstream path, utilities send operational commands to smart meters for two-way communication applications.

At present, the AMI two-way communication is being implemented by a variety of wired and wireless communication technologies. Those communication technologies are well reviewed in the literature [11], [14], [15]. Fiber-optic networks and WMNs are common choices for the first and the second layers of the AMI network, respectively. While other networks are also selected by utilities based on their needs on the network bandwidth, latency, cost, coverage, spectrum availability, cybersecurity, etc.

B. Industrial Practice

Starting from 2006, the Federal Energy Regulatory Commission (FERC) publishes annual reports to assess advanced

metering and demand response programs in the U.S. It is found that, originally, the AMI two-way communication was mainly developed to send time-based rates to customers to support demand response programs (i.e., billing purpose), but recently the two-way communication has been increasingly deployed to send control commands to smart meters and smart devices to support advanced applications (i.e., beyond billing purposes) [13]. Moreover, in 2019, the U.S. Department of Energy surveyed 120 electric utilities about their AMI applications beyond billing purposes. The survey shows that AMI has been successfully developed and demonstrated for monitoring and managing operating conditions, outage monitoring and management, DERs monitoring and management, asset monitoring and diagnostics, etc. [14].

In specific, Commonwealth Edison, Duke Energy, and several other utility companies utilize the smart meter pinging functionality to detect the operational status of certain distribution-level devices and then determine the cause and location of outages [14], [15]. For example, when there is an outage, the utility can ping a single smart meter to detect the energized status of the meter such that determine the outage cause (e.g., a response from the meter indicates the outage is a customer issue, such as tripped breakers, whereas no response from the meter indicates the outage is a system issue, such as damaged transformers); and the utility can also ping a batch of smart meters to identify outage locations or boundaries and verify restoration completeness. This is especially helpful in identifying whether the nested outage (e.g., a smaller outage nested within a larger outage) has been cleared up and whether the restoration to specific customers has been completed.

Pacific Gas and Electric Company (PG&E) plays a pioneering role in leveraging the AMI network to monitor and manage grid edge devices and DERs. Recently, PG&E used smart meters' voltage reading functionality to identify customer-owned DERs that were causing voltage deviation, and also utilized smart meter data in hosting capacity studies, helping PG&E determine allowable DER capacity to the system. PG&E successfully demonstrated the AMI capability that monitors, communicates with, and controls various end devices, such as smart inverters and DER controllers, over the existing AMI network with the IEEE 2030.5 protocol [17].

III. Model of AMI Communication Network

From 2006 to now, the applications of the AMI two-way communication have been extended from the billing purpose to the monitoring and management purpose. Some of the new applications, such as outage management and DER management, have QoS requirements on the communication network. Thus, it is advantageous to investigate the AMI network performance under the new applications.

Fig. 2. A tree structure model.

As aforementioned, there are two layers of the AMI network. In the first layer, optical fibers are typically used to directly connect the cell towers to the control center. This work is mainly focused on the second layer since it is involved with a large amount of intermediate data collection points with complex dynamics. In this section, a tree-based model of the AMI second layer (i.e., AMI WMN) is provided.

An AMI WMN logically can be treated as a tree network as shown in Fig. 2. The root node of the tree network refers to a cell tower and its children nodes (i.e., relay nodes) refer to cell relays. Each relay node has a number of immediate children nodes (i.e., meter nodes), and each meter node may also have its children nodes (this relation may further extend). Also, each link is a wireless link, where the wireless channel may be shared by multiple nodes, using certain MAC mechanisms. Briefly, the contention-based MAC works as follows. When a packet reaches the head of the queue at a node, sensing is performed and the packet is sent to the channel when the channel is sensed idle for a defined duration and the backoff countdown has reached zero. There are multiple backoff stages, each has a different initial value for backoff countdown. The packet is dropped if it does not get sent when the highest backoff stage is reached. Though different in some specific details, the essence of this medium access and backoff procedure is adopted by Wi-Fi (802.11), 802.15.4 (LR-WPAN), and 802.16 (Wi-MAX). Here, carrier-sense multiple access with collision avoidance (CSMA/CA) MAC is used between the cell tower and relay nodes, as well as within each relay node cell.

Also, in the tree network, all meter nodes under the same relay node are said to belong to the cell of this relay node. We assume that the network has been planned such that the meter nodes with different parent nodes do not interfere during their transmission. This includes two cases. One is that the meter nodes in different relay node cells do not interfere. Another one is that, even though they are within the same relay node cell, if a customer node's parent node is different from another one's, the two nodes do not interfere. We also practically assume that the transmission between the cell tower and relay nodes is independent of the transmission among the relay nodes and meter nodes.

Note that when a meter node relays traffic from other meter nodes towards the root, all meter nodes may need to compete to use the same wireless channel. An implication is that, if a meter node is used as a relay, its transmission not only needs to compete for the channel with its own child nodes but also with its sibling and parent meter nodes.

IV. Performance Analysis of AMI Communication Network

The end-to-end time delay is an important parameter to assess the AMI WMN performance. In this section, a network calculus-inspired approach is developed to calculate the delay between the cell tower and smart meters.

A. Key Ideas for the Analysis

Network calculus, as a queuing theory for performance guarantee analysis of computer networks, was first introduced

by Cruz for modeling network entities and flows [21], [24]. In the past two decades, it has been generalized by making use of alternate algebras such as min-plus and max-plus algebra to transform complex network systems into analytically tractable systems [21]–[24].

For delay bound analysis of WMNs, if the capacity of each link is dedicated and deterministically upper-bounded and the traffic is also upper-bounded, the network calculus-based analysis approach or procedure used for some existing network scenarios, e.g., [25], may be adapted. However, when the link is only logic and its characteristic is affected both by its corresponding wireless channel and by other users sharing the channel, to the best of our knowledge, no delay bound analysis, either based on network calculus or queuing theory, is immediately applicable for WMNs. Particularly, when the sharing of the wireless channel is contention-based, e.g. CSMA, even for the single-cell case, the analysis is already formidable, e.g., [26], [27], and additionally when one user is acting as the relay for other users, the analysis becomes more complex, e.g., [28], [29]. In the following, we outline some key ideas for the delay analysis.

- On both the upstream and the downstream paths, the end-to-end delay consists of two parts. One is the delay between the cell tower and the corresponding relay node, and another is the delay between the corresponding relay node and the meter node. The latter can be further decomposed into the delay on each hop, if other nodes are involved in forwarding, and the last hop is between the considered customer and the node that it connects to and forwards its traffic towards the root.
- For a node that helps relay traffic of other nodes, the traffic that is relayed by the node can be approximated as a Poisson process. This is from the result that, with CSMA with random backoff, the aggregate output process of packets from the users through the channel can be approximated as a Poisson process (see Theorem 1 in [26]). Note that such nodes include both the relay nodes and those nodes within each cell which have children nodes in the tree topology.
- For the last or first hop, e.g. from a customer node to its parent node on the upstream (e.g., meter reading) or from the cell tower to the relay nodes on the downstream (e.g., meter pinging), we assume that the traffic characterization is known, though it may not be Poisson.
- For each node, the service provided by the corresponding wireless channel to it can be characterized using a stochastic service curve (see Theorem 3 in [27]), which is a server model in stochastic network calculus. The results in [26], [27] essentially indicate that the delays of packets spent at the channel due to CSMA random backoff can be approximately viewed to follow an exponential distribution. Though the analysis in [26], [27] is for 802.11, similar observations are also found for 802.15.4 in an extensive experimental study [30].
- With the above traffic and service characterizations, the delay at each hop can be derived, based on which the end-to-end delay T_{e2e} is immediately obtained.

B. The Basics

1) A decomposition view of delay: Considering an AMI WMN with one root and N nodes, the upstream delay T_n^U of a packet from the node n $(n = 1, \ldots, N)$ to the root and the downstream delay T_n^D from the root to the node n can be simply written as the sum of the delay at each link:

$$T_n^U = T_{n\to r_{G-1}} + \sum_{g=1}^{G-2} T_{r_{g+1}\to r_g} + T_{r_1\to r_0} \quad (1)$$

$$T_n^D = T_{r_0\to r_1} + \sum_{g=1}^{G-2} T_{r_g\to r_{g+1}} + T_{r_{G-1}\to n} \quad (2)$$

where $x \to y$ refers to the link from node x to node y, and $T_{x\to y}$ refers to the delay on the link $x \to y$, with $x, y \in \{n, r_{G-1}, \ldots, r_1, r_0\}$. Here, r_0 denotes the root, r_g, $g = 1, \ldots, G-1$ denotes the nodes on the path between the root and node n, and G denotes the number of links on the path. On the upstream path $n \to r_0$, there are total G number of links, $n \to r_{G-1}, \ldots, r_1 \to r_0$, whereas on the downstream path $r_0 \to n$, there are also total G number of links, $\mathrm{r}_0 \to r_1$, $\ldots$, $r_{G-1} \to n$.

Both the upstream delay and the downstream delay consist of two components, the packet's waiting time in queue before the packet reaches the head-of-queue (HoQ) at each link, denoted as W_g on the g-th link, and the transmission time after the packet has reached the HoQ till it is successfully received, denoted as δ_g on the g-th link. Then the equations above can also be written as:

$$T_n^U = \sum_{g=1}^{G} W_g^U + \sum_{g=1}^{G} \delta_g^U \quad (3)$$

$$T_n^D = \sum_{g=1}^{G} W_g^D + \sum_{g=1}^{G} \delta_g^D \quad (4)$$

To simplify representation, the superscript U or D is omitted in the following discussion, but is clear from the context.

C. Best Case Delays (Minimum Delays)

Following (3) and (4), the minimum delay $T_{n,min}$ can be calculated with the maximum transmission rate of the g-th link R_g and the length of the packet l.

$$T_n \geq \sum_{g=1}^{G} \delta_g^D \geq \sum_{g=1}^{G} \frac{l}{R_g} \equiv T_{n,min} \quad (5)$$

This minimum delay can be reached when the traffic from other nodes on every link is so light that the link seems to be dedicated to the considered flow and when a packet arrives at every link seeing no previous packets from the same flow. Let us call the former the best condition. We are more interested in the maximum delay under the best condition, called the *best case maximum delay* $T_{n,bcm}$. As the discussion implies, it should only be affected by the traffic of the flow itself.

Suppose the amount of traffic generated by the customer node n in any period $[s,t]$, denoted as $A_n(s,t)$, is upper-bounded by a function, called arrival curve in network calculus, e.g., $A(s,t) \leq r(t-s)+b$. Then, the best case delay can be found from the network calculus analysis: if $r \leq \min_g R_g$,

$$T_{n,bcm} = \frac{b}{\min_{g=1}^{G} R_g} + \sum_{g=1, g\neq g'}^{G} \frac{l}{R_g} \quad (6)$$

where R_g denotes the data rate of the g-th link, and g' denotes the link whose data rate is $\min_g R_g$, implying it is the bottleneck link. The right hand side of (6) has two parts. Intuitively, the delay is composed of the transmission time of a packet on all other links (i.e., the second part), and the delay of the packet at the most congested link due to the traffic constraint condition (i.e., the first part).

D. Average Delays

Given (3) and (4), the average delay for the upstream traffic or downstream traffic of node n is simply

$$E[T]_n = \sum_{g=1}^{G} E[W]_g + \sum_{g=1}^{G} \bar{\delta}_g \quad (7)$$

where $\bar{\delta}_g$ denotes the mean of δ_g.

For all nodes under one relay node r, letting $\mathcal{N}_r$ denote the set of these nodes and N_r the number, their average delay is:

$$E[T]_r = \frac{\sum_{n\in\mathcal{N}_r} E[T]_n}{N_r} \quad (8)$$

Similarly, for all nodes in the network, letting $\mathcal{N}$ denote the set of nodes and N the number, the average delay is:

$$E[T] = \frac{\sum_{n\in\mathcal{N}} E[T]_n}{N} \quad (9)$$

E. Delay Bounds

1) A General Bound: Given (3) and (4), if the distribution of every W_g and δ_g is known, an upper bound on the distribution of T^U or T^D can be proved from the union bound:

$$P\{T_n > t\} \leq \inf_{\sum_{g=1}^{2G} p_g = 1} \sum_{g=1}^{G} \left[F^c_{W_g}(p_g t) + F^c_{\delta_g}(p_{G+g} t) \right] \quad (10)$$

for $\forall 0 < p_g < 1$, $g = 1, \ldots, 2G$, where $F^c_X(x)$ denotes the complimentary cumulative distribution function (CCDF) of random variable X, i.e., $F^c_X(x) \equiv P\{X > x\}$.

Note that the bound (10) is valid no matter if W_g and δ_g, for all $g = 1, \ldots, G$, are coupled or dependent.

2) An Improved Bound: Define the convolution operation $*$ of two distribution functions $F(t)$ and $G(t)$ as:

$$F * G(t) = \int_{-\infty}^{\infty} F(t-s) dG(s)$$

If W_g and δ_g, for all $g = 1, \ldots, G$, were independent on each other, improved bound on $P\{T > t\} \equiv F^c_T = 1 - F_T$ would be obtained by applying the fact that the sum of $2G$ random variables with a cumulative distribution function (CDF) $F_{W_1}, \ldots, F_{W_G}, F_{\delta_1}, \ldots, F_{\delta_g}$ has a CDF of the convolution of those probability density functions (pdfs), i.e., $F_T = F_{W_1} * \cdots * F_{W_G} * F_{\delta_1} * \cdots * F_{\delta_G}$. Hence,

$$P(T_n > t) = 1 - F_{W_1} * \cdots * F_{W_G} * F_{\delta_1} * \cdots * F_{\delta_G} \quad (11)$$

Note that, with the distribution bounds, bounds on the average delay can be immediately obtained, because $T_n \geq 0$ and hence

$$E[T_n] = \int_0^{\infty} P(T_n > t) dt$$

V. Case Studies

In this section, a set of case studies are carried out on the IEEE 13-node feeder and real-world feeder systems using ns-3 to verify the performances of the proposed methods.

A. Modified 13-Node Test Feeder

In IEEE Std. 1729-2014 IEEE Recommended Practice for Electric Power Distribution System Analysis, four small size distribution system models are recommended for test feeders, including 4, 13, 34, and 37 nodes test feeders [31]. Those test feeders provide complete models of medium-voltage and low-voltage distribution circuits for distribution system solutions testing, where a single electrical connection point is represented by a "node" and a set of electrical connection points at a geographic location is represented by a "bus". Due to the limited space, this paper only makes use of a modified 13-node test feeder as shown in Fig 3.

In the distribution domain, the original 13-node test feeder is a small radial distribution system including most of the common components deployed in actual distribution networks, such as voltage regulators, shunt capacitors, overhead and underground lines, and unbalanced loads. It has nine end-use loads with a peak load of 3.6 MVA (i.e., a highly loaded test feeder). The complete details can be found in [31]. Here, we assumed that each end-use load is connected with one residential network through a single-phase distribution transformer, and each residential network consists of different numbers of household customers as shown in Table I.

In the communication domain, the corresponding communication network includes a cell tower, nine cell relays, and a set of smart meters. It is assumed that each end-use load has been installed a cell relay and each household customer has its own smart meter. Also, the communication between the cell tower and cell relay follows IEEE 802.16 (WiMAX) and the communication of the mesh network follows IEEE 802.15.4. Both networks adopt CSMA for MAC. Other important communication parameters can be found in Tables II.

In Case 1, smart meters are required to report energy consumption in the past 8 hours within the next 5 hours. To avoid burst traffic, each meter randomly picks a starting time to transmit the data in a 5-hour window. In Case 2, the smart meters are requested to report energy consumption along with DER voltages. This means the payload data size becomes greater to carry the voltage readings at each meter location. The time window for transmitting meter data is still 5 hours.

In both cases, a single meter read consists of multiple network packets. It is viewed as a failed meter read if any of the packets does not reach the communication tower.

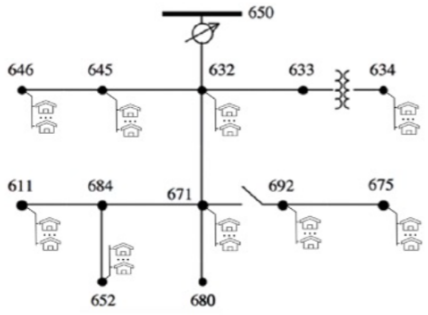

Fig. 3. Modified 13-Node Test Feeder

TABLE I
PARAMETERS OF AMI NETWORK

Node	Number of End-User	Phase
634	48	ABC
645	16	B
646	24	B
652	11	A
671	151	ABC
675	108	ABC
692	16	C
611	16	C
632	83	ABC

First, we examine the end-to-end delay between the cell relay and the smart meter. In terms of Case 1, the minimum and average delays using the network calculus method and the minimum and average delays using the ns-3 simulation are presented in Table III and Fig. 4, respectively. The detailed calculation of the network calculus can be found in Appendix. It is observed that the delay results through the network calculus and the simulation are consistent, validating the effectiveness of the proposed two-way communication model and network calculus method.

TABLE II
PARAMETERS OF TRAFFIC PATTERNS

Item	Case 1	Case 2
Data Time Window	8 hours	24 hours
Sending Time Window	5 hours	5 hours
Number of Packet for Single Read	2	6
Size per Packet	600 bytes	700 bytes

TABLE III
CALCULATION RESULTS OF CASE 1

Cell Relay Index	Node	Minimum Delay (ms)	Average Delay (ms)
1	634	39.4	122.8
2	645	39.4	40.3
3	646	39.4	52.0
4	652	39.4	40.3
5	671	39.4	144.0
6	675	39.4	130.4
7	692	39.4	40.3
8	611	39.4	40.3
9	632	39.4	182.7
10	633	39.4	112.2
11	680	39.4	104.5
12	684	39.4	158.3

Next, we evaluate the impact of DER monitoring on the AMI network. In Case 2, the smart meter is assumed to add DER measurements to smart meter readings such that the size of a smart meter message increases to 700*6 bytes, instead of 600*2 bytes. In addition, the smart meter is applied with heavier network traffic, where each smart meter is requested to send the meter reading every 24 hours, instead of 8 hours. The corresponding simulation results are presented in Fig. 5. It is shown that compared with Case 1, the end-to-end delays in Case 2 increase slightly. Those simulation results suggest that the AMI network configures with high bandwidth and the DER monitoring brings low impact on the AMI network. The DER monitoring is feasible for this AMI network.

Moreover, in both Figs 4 and 5, the average tree depth of each cell relay group is provided, representing the average packet hop counts that smart meter messages are transmitted to the corresponding cell relays. It is found that the average tree depth has a proportional relationship with the delay. This is because the actual number of hops in each cell relay group directly affects the maximum and average delays.

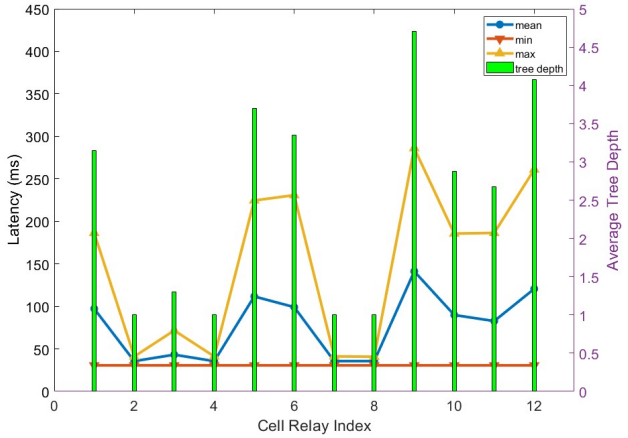

Fig. 4. Simulation results of Case 1.

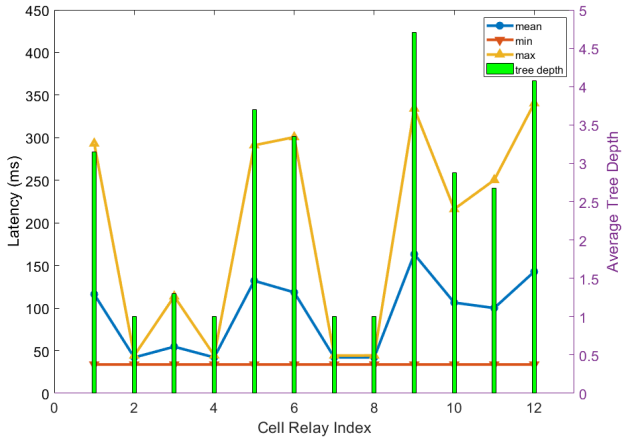

Fig. 5. Simulation results of Case 2.

B. Real-World Feeder

Several recent papers point out that the existing test systems typically cover only small portions of distribution circuits. The small- and medium-size test systems may not thoughtfully verify the new resolutions in face of the real complex cyber-physical systems [31]. An accurate scale-up of simulation techniques is critical for real-world application. To this end, a large real-world test system is employed here.

The parameters of the real-world test system are obtained from a research project through collaboration with an electric utility company in the U.S. The AMI network topology is similar to the one in Fig 1. The WiMAX network and the mesh network have bandwidth of 5Mbps and 250Kbps, respectively. The mesh network includes 24,413 smart meters and 72 cell relays.

With the large real-world test system, Cases 1 and 2 are repeated as Cases 3 and 4. The corresponding simulation results via ns-3 are shown in Figs. 6 and 7. We found that the distribution of the delays in Cases 3 and 4 is similar to that of Cases 1 and 2. In addition to the delay, we also observed the bandwidth usage using throughout as an indicator as shown in Fig .8. This result not only indicates the bandwidth usage of the AMI network but also implies the likelihood of traffic congestion between a cell relay and a smart meter. Those results suggest that the AMI network has additional bandwidth available, which allows the AMI network to communicate with and control DERs, such as solar PV and smart inverters.

In engineering, high communication delay increases the packet loss rate due to timeout errors, and the high packet loss rate directly impacts the delivery of smart meters' readings. Thus, it is important to study the smart meter packet behaviors and AMI network performances for different smart meter applications over different AMI networks. The proposed network calculus and the ns-3 simulation can help utilities investigate their AMI network performances (e.g., whether the average end-to-end delay and package loss rate meet the requirements of time-critical applications). The proposed studies can also help engineers identify the bandwidth usage and the weakest link and ultimately better make investment decisions.

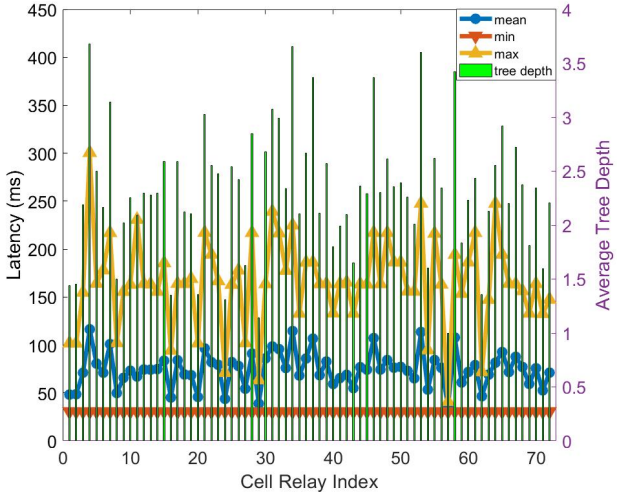

Fig. 6. Simulation results of Case 3.

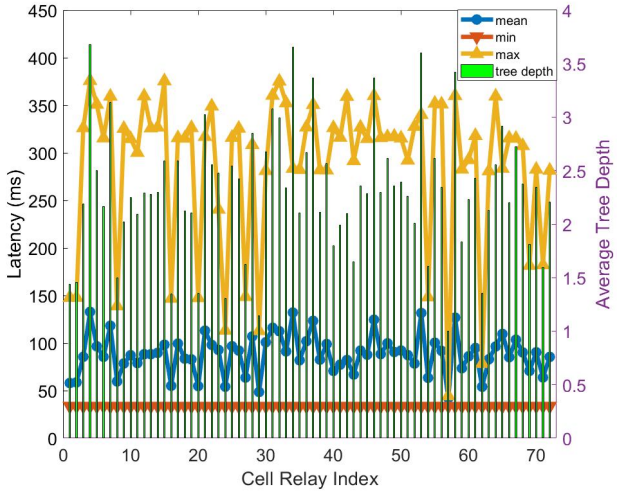

Fig. 7. Simulation results of Case 4.

VI. Conclusion

Today's power distribution system is changing to a power-electronics-enabled distribution system, especially with the increasing penetration of DERs. To monitor and manage those power electronic devices and DERs at the grid edge, smart meters-based AMI networks present great potentials, since they are the only networks that are widely deployed between electric utilities and end users and allowing two-way communications. This paper discussed the AMI two-way communication and its recent industrial practice in the U.S., especially the ones about applying smart meter pinging function to monitor grid edge devices and DERs. This paper then developed the two-way communication model and the network calculus method to quantify the impact of the two-way communication on the AMI network. In the end, the proposed method is validated with ns-3 simulation using the modified 13-node test feeder and real-world feeder systems.

Future work could include incorporating the proposed ns-3 model and network calculus method to the open-source co-simulation platform called Hierarchical Engine for Large-scale Infrastructure Co-Simulation (HELICS), and investigating the interaction between the two-way communication and distribution systems.

Acknowledgment

This work was sponsored by the Transactive Energy, Communications, and Interoperability in Smart Grid program under the U.S. Department of Energy's Office of Electricity. This work was performed under the auspices of the U.S. Department of Energy by Lawrence Livermore National Laboratory under Contract DE-AC52-07NA27344 with Release Number LLNL-JRNL-828091.

Appendix

We provide some examples of applying the network calculus method to calculate the delay.

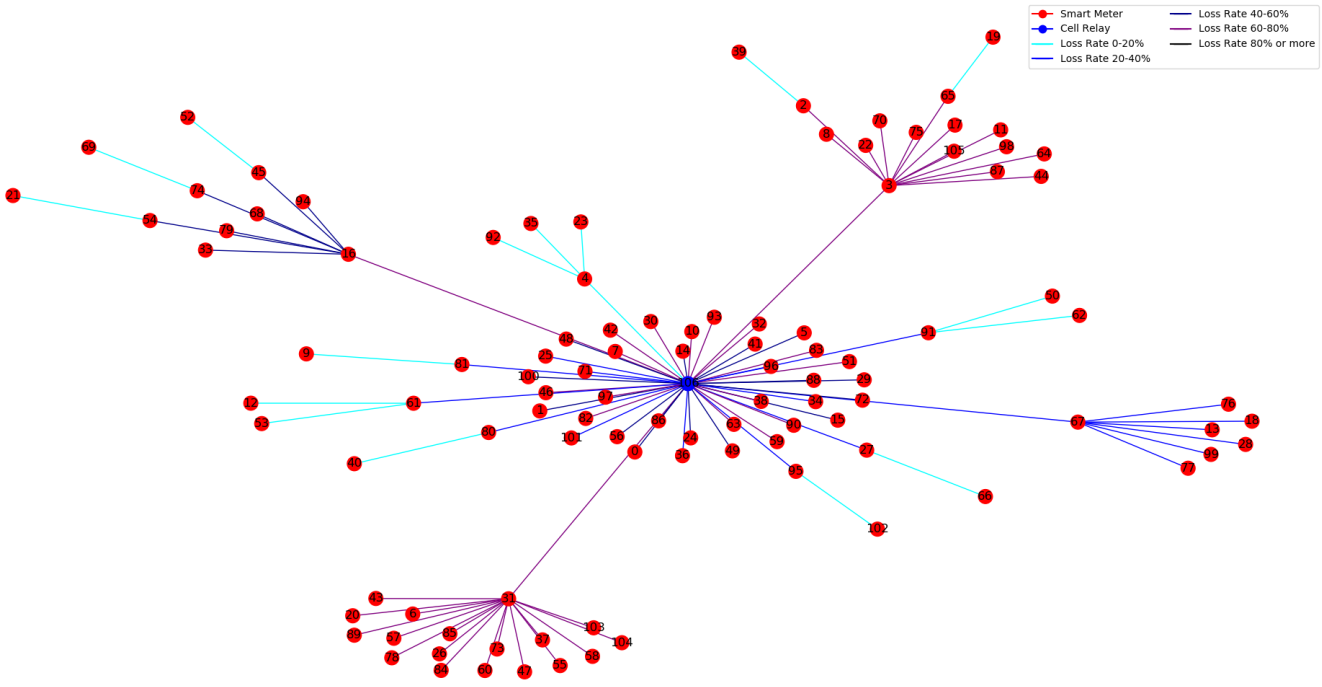

Fig. 8. Test results of bandwidth usage.

A. The Setting (Case 1)

Considering an AMI network as shown in Fig.s 1 and 2, the wireless channel for nodes under each relay node has a bandwidth of $250kbps$ and the channel between the cell tower and the relay nodes a bandwidth of $5Mbps$. In other words, the service rate of each channel is: $R_g = 250$ kbps, for $g = 1, \ldots, G-1$, and $R_G = 5Mbps$.

There are 12 cell relay nodes, where 9 of them directly connect 473 end users. There are 485 smart meters (473 at end users + 12 at cell relays). In other words, $N = 485$, and $N_r = N_{end-users} + 1$, where $N_{end-users}$ denotes the number of end-users under cell node r.

In Case 1, smart meters are required to report energy consumption in the past 8 hours within the next 5 hours. To avoid burst traffic, each meter randomly picks a starting time to transmit the data in a 5-hour window. The number of data packages for a single meter read is 2, where the size of each is $600bytes$. It is viewed as a failed meter read if any of these packages do not reach the cell tower. For this reason, we take l as the size of the message batch, i.e., $l = 1200bytes$.

The data rate per customer/smart meter is 2 packets every 8 hours, yielding $\lambda = 0.25$ pph (packets per hour) = $1/14400$ pps (packets per second) and $r = 1/3$ bps.

In addition, the traffic generated by the meter is upper bounded $A(s,t) \leq r(t-s) + b$ with $b = 2$ messages = $1200bytes$. The service rate of each channel is $\mu_{n\to r} = 250Kbps/4800bpp = 187.5Kpps$ (packets per second), for $g = 1, \ldots, G$ and $\mu_{r\to 0} = 20\mu_{n\to r}$ pps for $g = G$.

B. Best Case Delay (Minimum Delay)

For customer nodes under each cell relay, the best case is that the smart meter is an immediate child node of the relay node. In this case, $G = 2$; $R_1 = 250Kbps$, $R_2 = 5Mbps$; $b = 1200bytes$. Then, following (6), the minimum $T_{n,bcm}$ on the upstream is:

$$b/R_1 + l/R_2 \approx 39.4ms.$$

C. Average Delay

In [26], cf. Theorem 1, it has been shown that under CSMA/CA, the aggregate packet process by the users through the channel can be approximated as a Poisson process. In addition, according to the investigation in [27], δ is approximately exponentially-distributed.

We use (7) to find an estimate. Specifically, since all nodes under the same cell relay compete on the same channel, we simplify (7) for a customer node n:

$$E[T]_n = E[W]_{n\to r} + E[W]_{r\to 0} + \sum_{g=1}^{G} \bar{\delta}_g \quad (12)$$

$$E[W]_{n\to r} = \frac{\rho_{n\to r}}{\mu_{n\to r} - 2N_r\lambda} \quad (13)$$

$$E[W]_{r\to 0} = \frac{\rho_{r\to 0}}{\mu_{r\to 0} - N\lambda} \quad (14)$$

$$\bar{\delta}_g = \frac{l}{R_g} \quad (15)$$

with $\rho_{n\to r} \equiv 2N_r\lambda/\mu_{n\to r}$ and $\rho_{r\to 0} \equiv N\lambda/\mu_{r\to 0}$, where $E[W]$ is approximated from $M/M/1$ queuing analysis. The alert reader may have noticed that on the right hand side of (12), and the path from n to the relay r is only treated as if there were only one queue, instead of $G-1$ queues. This approximation can be verified using stochastic network calculus analysis technique [24].

As a highlight, the total packet rate to the link $n \to r$ is twice the total packet rate of all customer nodes under the relay r in (13). This is because, after receiving the packets from all the smart meters, the relay node still needs to relay them to the cell tower via the same channel.

For a more specific example, consider one user node / smart meter under the relay with 151 end users (cf. Table I), and suppose for this node $G = 5$, i.e., tree depth is about 4 in Fig. 4. Then, $\mu_{n\to r} \approx 52$ pps (packets per second), and $2N_r\lambda \approx 0.02$ pps.

$$E[W]_{n\to r} = \frac{0.02/52}{52 - 0.02} seconds < 1ms \quad (16)$$

$$E[W]_{r\to 0} = \frac{\rho_{r\to 0}}{\mu_{r\to 0} - N\lambda} < 1ms \quad (17)$$

$$\bar{\delta}_g = \frac{l}{R_g} \approx 38.5ms, \quad 1 \le g < G \quad (18)$$

$$\bar{\delta}_G = \frac{l}{R_G} \approx 2ms \quad (19)$$

Hence, for this node, the expected delay is:

$$E[T]_n = E[W]_{n\to r} + E[W]_{r\to 0} + 4\bar{\delta}_g + \bar{\delta}_G \approx 156ms$$

Note that in the calculation in Table III, in terms of the cell relay #5, the average tree depth is 3.7 and thus the corresponding average delay is $144ms$, instead of $156ms$.

D. Delay Distribution Bounds

Following the same analogy, we simplify (3) or (4) and use:

$$T_n = W_{c\to r} + W_{r\to 0} + \sum_{g=1}^{G} \delta_g \quad (20)$$

For δ_g, according to the investigation in [27], it is approximately exponentially-distributed, i.e.,

$$P\{\delta_g > t\} \le e^{-\bar{\delta}_g t} \quad (21)$$

For waiting time in a system, such as $W_{c\to r}$ and $W_{r\to 0}$, various bounds are proved in [24]. In particular, corresponding to the two cases, i.e., i.i.d. Poisson arrival or periodic arrival and i.i.d. exponentially distributed service time, the following bound has been proved [24]:

$$P\{W_g > t\} \le e^{-\nu_g t} \quad (22)$$

with $\nu_g = \mu_g - \lambda_g$ and g representing the corresponding hop of $c \to r$ or $r \to 0$.

Applying the above, the distribution bounds (10) and (11) can be simplified and calculated.

REFERENCES

[1] B. Chen, J. Wang, X. Lu, C. Chen, and S. Zhao, "Networked microgrids for grid resilience, robustness, and efficiency: A review," *IEEE Trans. Smart Grid*, vol. 12, no. 1, pp. 18-32, Jan. 2021.

[2] F. Shen, Q. Wu, and Y. Xue, "Review of service restoration for distribution networks," *J. Mod. Power Syst. Clean Energy*, vol. 8, no. 1, pp. 1-14, Jan. 2020.

[3] K. Ahmed, M. Seyedmahmoudian, S. Mekhilef, N. M. Mubarak, and A. Stojcevski, "A review on primary and secondary controls of inverter-interfaced microgrid," *J. Mod. Power Syst. Clean Energy*, vol. 9, no. 5, pp. 969-985, Sep. 2021.

[4] F. Li et al., "Review of real-time simulation of power electronics," *J. Mod. Power Syst. Clean Energy*, vol. 8, no. 4, pp. 796-808, July 2020.

[5] S. Peyghami, P. Palensky, M. Fotuhi-Firuzabad, and F. Blaabjerg, "System-level design for reliability and maintenance scheduling in modern power electronic-based power systems," *IEEE Open Access J. Power Energy*, vol. 7, pp. 414-429, 2020.

[6] R. Kenyon, J. Maguire, E. Present, D. Christensen, and B. -M. Hodge, "Bulk electric power system risks from coordinated edge devices," *IEEE Open Access J. Power Energy*, vol. 8, pp. 35-44, 2021.

[7] I. Kosen et al., "UPS: Unified PMU-data storage system to enhance T+D PMU data usability," *IEEE Trans. Smart Grid*, vol. 11, no. 1, pp. 739-748, Jan. 2020.

[8] J. Zhao, C. Huang, L. Mili, Y. Zhang, and L. Min, "Robust medium voltage distribution system state estimation using multi-source data," *2020 IEEE Power Energy Society Innovative Smart Grid Technologies Conference (ISGT)*, pp. 1–5.

[9] C. Huang et al., "Power distribution system synchrophasor measurements with non-Gaussian noises: Real-World data testing and analysis," *IEEE Open Access J. Power Energy*, vol. 8, pp. 223-228, 2021.

[10] N. Duan, C. Huang, C. -C. Sun, and L. Min, "Smart meters enabling voltage monitoring and control: The last-mile voltage stability issue," *IEEE Trans. Ind. Informat.*, vol. 18, no. 1, pp. 677-687, Jan. 2022.

[11] A. Ghosal and M. Conti, "Key management systems for smart grid advanced metering infrastructure: A survey," *IEEE Commun. SurveysTuts.*, vol. 21, no. 3, pp. 2831–2848, 3rd Quart., 2019.

[12] Y. Wang, Q. Chen, T. Hong, and C. Kang, "Review of smart meter data analytics: Applications, methodologies, and challenges," *IEEE Trans. Smart Grid*, vol. 10, no. 3, pp. 3125–3148, May 2019.

[13] The U.S. Federal Energy Regulatory Commission Staff Team, *Assessment of Demand Response and Advanced Metering*, Dec. 2020.

[14] The U.S. Department of Energy, *Voice of Experience: Leveraging AMI Networks and Data*, Mar. 2019.

[15] The U.S. Department of Energy, *Advanced Metering Infrastructure and Customer Systems*, Dec. 2016.

[16] B. Palmintier, D. Krishnamurthy, P. Top, S. Smith, J. Daily, and J. Fuller, "Design of the HELICS high-performance transmission-distribution-communication-market co-simulation framework," *2017 Workshop on Modeling and Simulation of Cyber-Physical Energy Systems (MSCPES)*, pp. 1-6.

[17] Pacific Gas and Electric Company, *EPIC Final Report - 2.26, Customer and Distribution Automation Open Architecture Devices*, 2019.

[18] Z. Liang et al., "Safe reinforcement learning-based resilient proactive scheduling for a commercial building considering correlated demand response,"*IEEE Open Access J. Power Energy*, vol. 8, pp. 85-96, 2021.

[19] B. Zhou et al., "Multi-microgrid energy management systems: Architecture, communication, and scheduling strategies," *J. Mod. Power Syst. Clean Energy*, vol. 9, no. 3, pp. 463-476, May 2021.

[20] W. Zheng, Z. Li, X. Liang, J. Zheng, Q. H. Wu, and F. Hu, "Decentralized state estimation of combined heat and power system considering communication packet loss," *J. Mod. Power Syst. Clean Energy*, vol. 8, no. 4, pp. 646-656, July 2020.

[21] R. L. Cruz. "A calculus for network delay, part I and part II," *IEEE Trans. Inf. Theory*, vol. 37, no. 1, pp. 114–141, Jan. 1991.

[22] J.-Y. Le Boudec and P. Thiran, *Network Calculus: A Theory of Deterministic Queueing Systems for the Internet*, Springer-Verlag, 2001.

[23] Y. Jiang and Y. Liu, *Stochastic Network Calculus*, Springer, 2008.

[24] Y. Jiang, "Network calculus and queueing theory: two sides of one coin," *Proc. of 4th International Conference on Performance Evaluation Methodologies and Tools (VALUETOOLS)*, 2009, pp. 1-11.

[25] C Huang, F Li, T Ding, Y Jiang, J Guo, and Y Liu, "A bounded model of the communication delay for system integrity protection schemes," *IEEE Trans. Power Deliv.*, vol. 31, no. 4, 1921-1933, Aug. 2016.

[26] J. Cho and Y. Jiang, "Fundamentals of the backoff process in 802.11: Dichotomy of the aggregation," *IEEE Trans. Info. Theory*, vol. 61, no. 4, pp. 1687-1701, April 2015.

[27] M. Bredel and M. Fidler, "Understanding fairness and its impact on quality of service in IEEE 802.11," *2009 IEEE INFOCOM*, pp. 1098–1106.

[28] F. Ciucu, R. Khalili, Y. Jiang, L. Yang, Y. Cui, "Towards a system theoretic approach to wireless network capacity in finite time and space," *2014 IEEE INFOCOM*, pp. 2391-2399.

[29] F. Sun and Y. Jiang, "A statistical property of wireless channel capacity: Theory and application," *ACM SIGMETRICS Performance Evaluation Review*, vol. 45, no. 3, pp. 97-108, Dec. 2017.
[30] S. Fu, Y. Zhang, M. Ceriotti, Y. Jiang, M. Packeiser, and P. J. Marrón, "Modeling packet loss rate of IEEE 802.15.4 links in diverse environmental conditions," *2018 IEEE Wireless Communications and Networking Conference (WCNC)*, pp. 1-6.
[31] F. E. P. Marcos et al., "A review of power distribution test feeders in the United States and the need for synthetic representative networks," *Energies*, vol. 10, no. 11, pp. 1896-1910, Nov. 2017.

Can Huang (S'13–M'16–SM'18) received the B.S.E.E degree from Hohai University, Nanjing, China, in 2008, the M.S.E.E. degree from Southeast University, Nanjing, China, in 2011, and the Ph.D. degree in electrical engineering from the University of Tennessee, Knoxville, TN, USA, in 2016. Now he is a research staff with Lawrence Livermore National Laboratory, Livermore, CA, USA. His current research interests include smart sensors, data analytics, and machine learning for energy and power systems, cyber-physical systems, and Internet of Things.

Chih-Che Sun (S'15-M'20) received the Ph.D. degree in electrical engineering from the Washington State University, Pullman, WA, USA, in 2019. He is currently a postdoctoral research staff with Lawrence Livermore National Laboratory, Livermore, CA, USA. His current research interests include cyber-physical systems (CPS) security, and their modeling and simulation.

Nan Duan (S'14–M'18–SM'20) received his B.S. in automation from Beijing University of Technology, Beijing, China, M.Eng. in control engineering from Beihang University, Beijing, China and Ph.D. in electrical engineering from the University of Tennessee, Knoxville, TN, USA, in 2010, 2013 and 2018, respectively. He is currently a power systems engineer with Lawrence Livermore National Laboratory, CA, USA. His research interests include power system modeling, high-performance computing, machine learning, and synchrophasor applications.

Yuming Jiang (SM'14) received the B.Sc. degree in electronic engineering from Peking University, Beijing, China, in 1988, the M.Eng. degree in computer science and engineering from Beijing Institute of Technology, Beijing, China, in 1991, and the Ph.D. degree in electrical and computer engineering from the National University of Singapore, Singapore, in 2001. He has been a Professor with the Norwegian University of Science and Technology, Trondheim, Norway, since 2005. From 1996 to 1997, he was with Motorola, Beijing, China, and from 2001 to 2003, he was with the Institute for Infocomm Research (I2R), Singapore. He visited Northwestern University from 2009 to 2010, and Columbia University from 2015 to 2016. He has authored the book entitled Stochastic Network Calculus. His research interests are the provision, analysis, and management of quality of service guarantees, with a focus on (stochastic) network calculus and its applications. He was a Co-Chair of IEEE Globecom 2005—General Conference Symposium, a TPC Co-Chair of 67th IEEE Vehicular Technology Conference 2008, the General Chair of IFIP Networking 2014 Conference, the Chair of the 2018 International Workshop on Network Calculus and Applications, and a TPC Co-Chair of the 32nd International Teletraffic Congress, 2020.

Chloe Applegate received the M.S. and Ph.D. degrees in civil engineering from Georgia Institute of Technology, Atlanta, GA, USA, in 2018. She is currently a Systems Analyst and the Deputy Associate Program Leader for Cyber Systems Analysis at Lawrence Livermore National Laboratory, Livermore, CA, USA. She works primarily on developing methods to compare risk across infrastructure systems and analyze infrastructure system interdependence.

Peter D. Barnes received the Ph.D. degree in Physics from the University of California, Berkeley, CA, USA, in 1996. He currently leads the Network Simulation team at Lawrence Livermore National Laboratory, Livermore, CA, USA. His current research interests include the scaling of simulation models to very large sizes to be executed in parallel on extreme scale parallel processing hardware.

Emma Stewart (M'08–SM'14) received the M.S. and Ph.D. degrees in electrical engineering from the University of Strathclyde, Glasgow, U.K., in 2004 and 2009, respectively. She is currently the Chief Scientist with the National Rural Electric Cooperative Association (NRECA), USA. Before joining the NRECA, her previous positions include the Associate Program Leader of the Defense Infrastructure area at the Lawrence Livermore National Laboratory, the Deputy Grid Integration Group Leader at the Lawrence Berkeley National Laboratory, a Senior Engineer at DNV Company, and a Visiting Researcher at the Sandia National Laboratory. She works primarily on leading the business technology strategies team to further advance research into grid resilience and reliability, transmission and distribution, and cybersecurity.